

Design and Construction of Novel Instrumentation for Low-Field MR Tomography

Daniel Gogola¹, Pavol Szomolanyi^{1,2}, Martin Škrátek¹, Ivan Frollo¹

¹*Institute of Measurement Science, Department of imaging method, Dúbravská cesta, 9, 841 04, Bratislava, Slovakia, daniel.gogola@savba.sk*

²*High Field MR Centre, Department of Biomedical Imaging and Image-guided Therapy, Medical University of Vienna, Vienna General Hospital, Waehringer Guertel 18-20, A-1090, Vienna, Austria*

Magnetic resonance imaging (MRI) is a very popular tool for diagnostic applications and research studies. Low-field MR scanners, usually with an open design, are suitable for claustrophobic and obese patients, as well as for children, who may be fearful in closed MR scanners. However, these types of scanners provide lower spatial resolution and a lower signal-to-noise ratio (SNR) if compared with the same examination performed at the same time at high field scanners. It is dominantly caused by the low field strength and other factors, such as radiofrequency noise. Therefore, a long measurement time is usually necessary. This research paper is focused on the development of novel probes and preamplifiers for low-field MR scanners to improve SNR, and thus, shorten the measurement time. In this study, we describe the design of a high impedance preamplifier and a high temperature superconductor (HTS) coil. This novel instrumentation was compared with uncooled and cooled copper coils. Improvement in SNR in the case of an HTS coil is reported.

Keywords: Imaging, MRI, low-field tomography, signal-to-noise ratio (SNR), probe, coils, preamplifiers.

1. INTRODUCTION

Signal-to-noise ratio (SNR) is one of the most important parameters for assessing the quality of images obtained by magnetic resonance imaging (MRI) in biomedical applications. Parameters such as spatial resolution and acquisition times are closely related to the SNR [1], [2], [3]. SNR is especially crucial at low fields, as the signal intensity is field-dependent. Although MR systems with high magnetic field strengths are the mainstream scanners these days, low-field systems are still commonly used, as they provide space and accessibility important for claustrophobic and obese patients, for example, as well as for children, who are often fearful in closed MR scanners. Low fields are also useful for modern applications, such as blood oxygenation level dependent contrast MRI (BOLD MRI) [4], [5] and are even more desirable than high fields in some special applications, e.g., hyperpolarized gas lung MRI [6], [7]. In these types of scanners, the SNR is usually increased through signal averaging, which also makes the examination time-demanding.

There are many sources of noise that reduce image quality. Some of the most important of these are sample noise, patient noise, amplifier noise, and internal noise caused by the receiving coil itself. Impact of these noise categories depends on operating frequency and coil size. Based on these parameters we can operate in the sample noise dominant

regime or in the coil noise dominant regime. Sample or patient noise are caused by the thermal (Brownian) motion of electrons within the body's conducting tissue. Brownian motion gives rise to random radiofrequency (RF) currents, organized in a number of round-shaped eddy current loops, when the sample is placed into the magnetic field. These current loops produce random changes in magnetic fields, thus inducing noise voltage in the receiving RF coil [8]. This source of noise is important for both high-field MR scanners and low-field scanners. The way to reduce the impact of this source of noise on the MR images is to reduce the receiver bandwidth around the observed Larmor frequency. This can be achieved with a receiving coil of the highest possible quality. The coil quality can be expressed as:

$$Q = \frac{f_0}{\Delta f} \quad (1)$$

where Q is the quality of the receiving coil (resonance circuit), f_0 is the Larmor (observed) frequency, and Δf is the bandwidth.

The second important source of noise is the noise produced by the receiving coil itself, sometimes called Johnson noise. The inherent coil noise can be reduced by cooling down the temperature of the receiving coil [9]. This will also improve the quality of the receiving coil through a bandwidth

reduction (1). To improve the SNR gain of the receiving coils, it is advantageous to use high temperature superconducting (HTS) materials for the construction of the receiving coils.

The dominant source of Johnson's noise at low frequencies can be the receiver [8]. Furthermore, low-field systems often use a resistive type magnet with a volume-limited homogeneous static magnetic field. For large diameter coils with large objects measured with the coil, the sample exceeds limited volume where B₀ homogeneity region is guaranteed. As a consequence, lower SNR is achieved.

The usual cooling method for the winding of HTS coils is immersion into liquid nitrogen. The reason liquid nitrogen is used is that its boiling temperature is 77 K, and therefore, it is easier to handle [8] than liquid helium.

Cooling of the coil causes a decrease in its resistance, together with the noise it causes. Closely linked with the decreased resistance of the coil windings is the improvement in the quality of the coil windings. The quality of the coil windings with serial resistance can be expressed as [10]:

$$Q_U = \frac{\omega_0 L}{R_C} \quad (2)$$

where Q_U is the quality of unloaded coil windings, ω_0 is the Larmor frequency, L is the inductance of the unloaded coil windings, and R_C is the resistance of unloaded coil windings. Improved SNR has been described [11] by the following formula:

$$SNR = \sqrt{\frac{Q_L}{T}} \quad (3)$$

where T is temperature of coil windings, and Q_L is quality of the coil loaded by the sample.

A common measure of probe performance is the ratio r between the Q factor of the unloaded and loaded coil (i.e., sensitivity to loading) described as follows [12]:

$$r = \frac{Q_U}{Q_L} = \frac{R_C + R_{SAMPLE}}{R_C} \quad (4)$$

Another property of the receiving coil that influences the SNR is the coil filling factor, η . This factor is defined as the fraction of RF energy created by the coil, which is stored in the sample volume [11]. The relation between the filling factor and SNR has been described [13] by the following formula:

$$SNR \propto \sqrt{\eta Q_L} \quad (5)$$

For the filling factor maximization, a volume coil is suitable. Due to the thermal isolation needed between the HTS coil and the sample, a slightly reduced filling factor is typical, which limits the potential SNR improvement [11]. Most recent studies have focused on the development of surface receiver coils for low-field scanners [14]. However, volume coils are still of great interest [15].

The aim of this work was to design novel measurement instrumentation, which consists of a volume coil and a preamplifier for low-field MRI systems. Such instrumentation will potentially provide better image quality, with higher SNR for future *in vitro*, as well as *in vivo* measurements, and for testing MR systems performance.

2. SUBJECT & METHODS

A. Design and construction of the HTS coil and pick-up loop

The receiving coil significantly affects the quality of images at low-field MR imaging. Thus, we designed the receiving coil in the form of a single-turn solenoid (volume coil), which has higher sensitivity compared to other single-turn volume receiving coils made of other conductive materials. The HTS receiving coil was built as a single loop (132 mm in diameter) of thin tape of bismuth strontium calcium copper oxide (BSCCO) with a width of 2.6 mm.

When the HTS coil is cooled to 77 K, the HTS windings have low resistance, and the impedance of the parallel resonance circuit is high. The cooled HTS coil had high frequency selectivity; therefore, it had to be precisely tuned to the Larmor frequency of the scanner, in our case, 7.605 MHz. For this purpose, the HTS coil was roughly tuned by fixed, high-quality capacitors and capacitance diodes were added for fine-tuning, as depicted in Fig. 1.

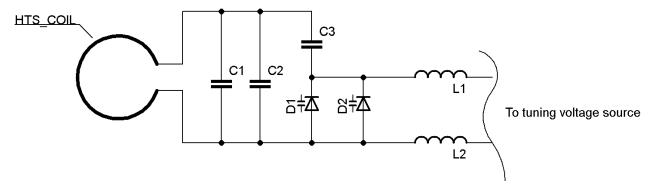


Fig.1. Schematic of HTS coil with fixed capacitors and with added capacitance diodes.

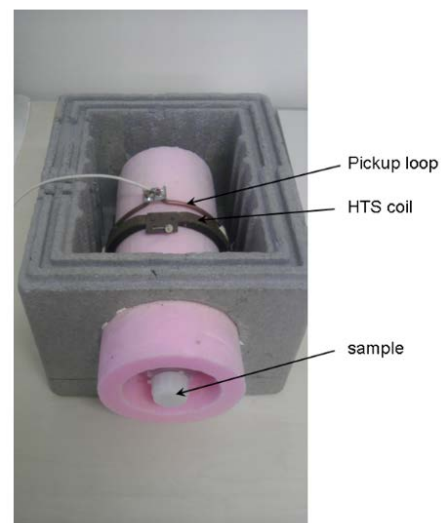


Fig.2. Cryostat with the HTS coil, the pickup loop and the sample. The sample consisted of a bottle with a water solution of 0.648 g/L NiCl₂ and 3.214 g/L NaCl.

At this resonance frequency, the skin effect of the material becomes significant; therefore, the thin silver tapes, originally molded to the BSCCO to increase the mechanical strength of the HTS tape, had to be removed by etching. The BSCCO loop modified in this way was placed into the cooling holder and attached there with epoxy glue.

As the HTS resonator has too high impedance at resonance frequency, and its direct connection to the preamplifier would cause an unwanted decrease in the quality of the HTS resonator, a pickup loop had to be used. The pickup loop was made of thin-wall copper tubing.

This loop was directly connected to the preamplifier without tuning. Impedance matching of the receiving HTS coil to the preamplifier was achieved by choosing an appropriate distance between the HTS coil and the pickup loop (Fig.2.).

B. Preamplifier

To achieve satisfactory SNR, the receive probe should be precisely tuned to the Larmor frequency of the MR scanner and matched to the transmission path. The classical approach is to tune the probe by two trimming capacitors that work as a tuning and matching set. This method is usually used when the probe is connected to the preamplifier by a coaxial cable, with a characteristic impedance of 50 Ohm. Another option for connecting the receive coil is to use a preamplifier with a high input impedance. Such a preamplifier can be directly connected as close as possible to the receive coil. In this case, the preamplifier must be constructed without magnetic components and the main magnetic field of the scanner must not interfere with its operation, e.g., amplification. The preamplifier circuit developed for our applications is shown in Fig.3.

This preamplifier can be directly (without coaxial cable) connected to the pickup loop. Given that the preamplifier has a high input impedance of 3.53 k Ω , the distance between the receiving coil (HTS coil) and the pickup loop was set to 1.5 cm, as determined experimentally. The output of this preamplifier was fixed by matching to a transmission line with characteristic impedance of 50 Ohm. In this way, the tuning of the probe was simplified, because it was sufficient to tune the probe to the resonance frequency, as no additional matching was required. The preamplifier was designed for low-field scanners, with the magnetic induction of the main field at 0.1 - 0.18 T. For protection of the signal input of the preamplifier, non-magnetic MELF (Metal Electrode Leadless Faced) diodes MADP-000235-10720T (M/A-COM Inc., Technology Solutions, Lowell, Massachusetts) were used. At the input of the preamplifier, two low-noise and high-linearity Pseudomorphic High Electron Mobility transistor (PHEMT) Field Effect Transistors (FET) transistors, ATF 34143 (Avago Technologies, San Jose, California), were used. The preamplifier was powered by the symmetrical voltage ± 5 V. Frequency selectivity of this preamplifier is given by the connected receiving coil and resonant coupling inside the preamplifier.

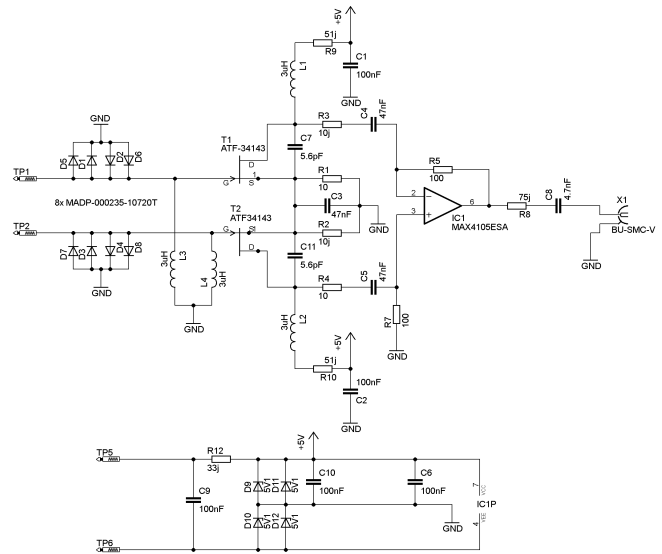


Fig.3. Schematic of high impedance differential preamplifier with power source.

C. Test of coil performance

HTS coil parameters (BW, Q) were measured outside the scanner by an impedance meter, TE 1000 RF (TOMCO Technologies, Norwood, Australia).

For comparison, the properties of the superconducting coil were compared with the properties of a standard copper coil constructed as a single loop of copper tape, 2.6 mm wide and 0.15 mm thick. The loop had the same diameter as the HTS coil, for direct comparison [15]. Properties of this copper coil were evaluated with and without nitrogen cooling.

The coils were also compared in terms of imaging performance, where the SNR was calculated for quantitative comparison. Both coils, HTS and copper, were placed into the same cryostat during imaging. The SNR was calculated (6) as the ratio between the mean signal intensity of a phantom image and the standard deviation of the background noise. A bottle phantom of 8 cm in diameter filled with a liquid solution containing 0.648 g/L NiCl₂ and 3.214 g/L NaCl in distilled water to mimic the body loading was used.

$$SNR = \frac{S_{mean}}{N_{S.D.}} \quad (6)$$

where S_{mean} is the mean value of the signal and $N_{S.D.}$ is the standard deviation of the noise background.

The phantom images were obtained by all three coils, using the developed preamplifier, on a 0.18 T MR scanner, the E-scan Opera (ESAOTE, Genoa, Italy). Equally set T₁-weighted spin echo images were obtained, with TE = 18 ms, TR = 500 ms, an acquisition matrix 256x256, number of acquisitions (NumAcq) = 1, and a slice thickness of 5 mm. The SNR was calculated from the signal intensity taken from an area of 1x1 cm in the center of the imaged phantom.

3. RESULTS

The images in Fig.6. were obtained to compare the impact of different coils on the image quality. The quality of the obtained images was based on the calculated SNR value.

The quality factors of HTS and copper coils were measured and compared. The detailed values of the coil properties are summarized in Table 1. A decrease in frequency bandwidth with increased quality of the coil was detected, which was in agreement with the expectations.

Table 1. Parameters of used coils.

Coil	State	Bandwidth [kHz]	Quality of loaded receiving coil	Quality of unloaded receiving coil	Filing factor [%]
copper	uncooled	118	64.5	64.5	58
copper	cooled	41	185	186	58
HTS	cooled	23	330	387.47	58

Fig.6. shows a large difference in image quality, if cooled and uncooled copper coils, respectively, were used for acquisition. The differences between the cooled copper coil and the HTS coil were not obvious to the naked eye, but the measured SNR was higher for the HTS coil.

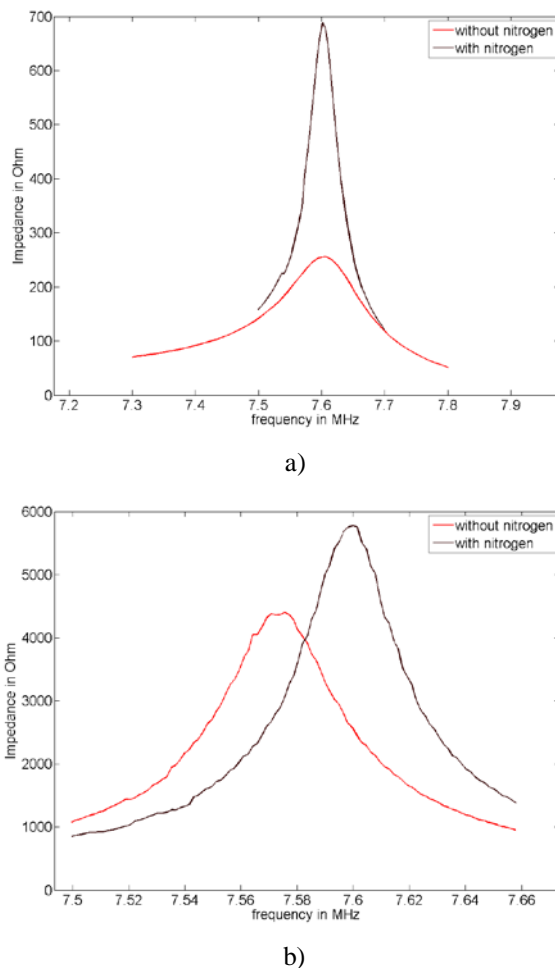


Fig.4. Impedance characteristic of a) copper coil and b) an HTS coil.

The SNR of the room-temperature copper coil was 14.53, while the SNR of the cooled copper coil was 38.75, equal to a 2.67 times greater SNR in the cooled state. For the HTS coil, the achieved SNR was 52.9, which is 3.6 times higher and 1.4 times higher than the SNR of the room-temperature and cooled copper coils, respectively. The loaded winding resistance, R_C , of both coils decreased after cooling with liquid nitrogen, which caused an increased impedance of the receiving resonance circuit (Fig.4.), and a corresponding increase in the quality of the coils (Table 1.), as described by equation (2). The induction of the HTS coil was changed after cooling, unlike the copper coil, as shown in Fig.4. The improvement in SNR can be calculated from equation (7), as a ratio of SNRs at room temperature and at the working temperature of liquid nitrogen, 77 K. Theoretically, the improvement in SNR (for the tested copper coil at 296.15 K room temperature) can be calculated as follows:

$$\frac{SNR_{77\text{ K}}}{SNR_{296.15\text{ K}}} = \sqrt{\frac{Q_{77\text{ K}} \cdot 296.15}{Q_{296.15\text{ K}} \cdot 77}} = 3.32 \quad (7)$$

4. DISCUSSION / CONCLUSIONS

Novel measurement instrumentation, with a high impedance preamplifier and a superconducting coil, was developed and tested on a clinical low-field scanner.

The preamplifier itself is broad-banded, as shown by amplitude frequency characteristic in Fig.5.

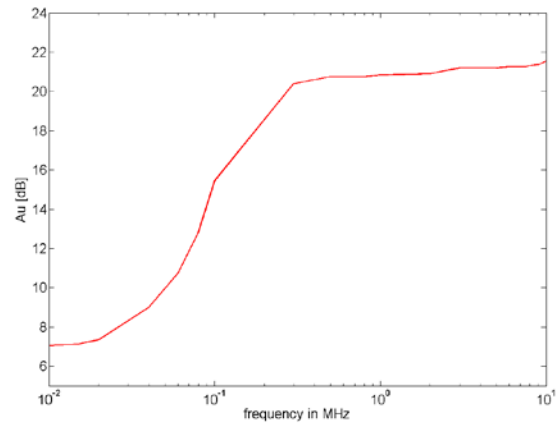


Fig.5. Amplitude frequency characteristic of preamplifier, measured without receiving coil.

Around the required frequency, which is 7.605 MHz (the Larmor frequency of hydrogen nucleus on a scanner with a main field of 0.18 T, which was the scanner we used), the gain of this designed and constructed preamplifier was 21.26 dB and the noise figure was 2.2 dB. The constructed preamplifier had acceptable parameters, which were independent of the magnetic field strength. The amplifier gain was independent relative to the B_0 field. It was identical inside and outside the main static magnetic field B_0 . The placement of the preamplifier into the B_0 static magnetic field had no effect on the image quality.

For comparison, two types of receiving coils were constructed, one of copper and one of BSCCO tapes. These coils were of the same circular geometry: 2.6 mm wide and 132 mm in diameter. The quality of the acquired images was evaluated on the basis of the achieved SNR. A relatively high change in SNR is obvious in Fig.6.a) and Fig.6.b). From the obtained images, it was calculated that the SNR improved 2.67 times after the copper coil was cooled (Fig.6.b). The theoretically calculated improvement in SNR was posited to be slightly higher (3.32) than the experimentally measured value. This was probably caused by the interference of the main static magnetic field of the tomograph with the impedance meter probe. Further improvement in SNR was achieved by using the HTS coil. The measured SNR was 3.64 times higher than the SNR for the uncooled copper coil. Compared to the cooled copper coil, SNR was further improved by a factor of 1.37.

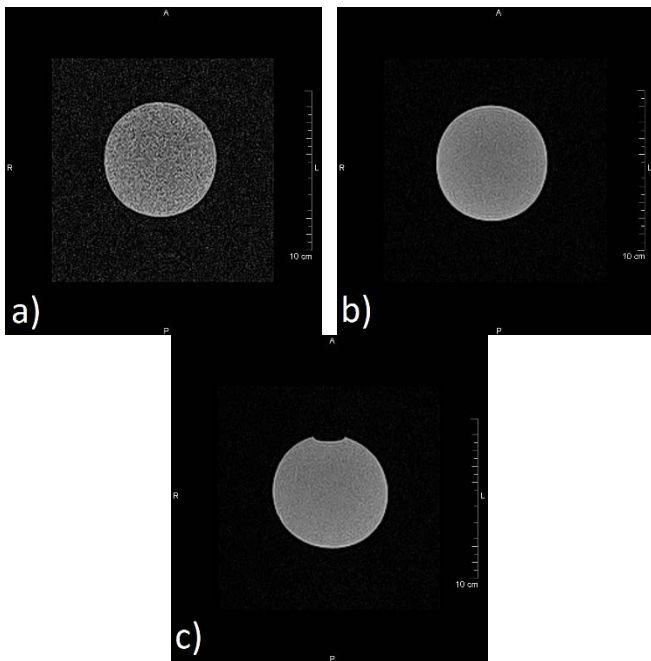


Fig.6. Images of the same slice of a water phantom: a) image obtained by uncooled copper coil, with the SNR = 14.53, b) image obtained by a cooled copper coil, with the SNR = 38.75, c) image obtained with an HTS coil, with the SNR = 52.9. An air bubble is visible in figure c, which had moved into this slice, causing an artifact, but this did not compromise the SNR evaluation.

This improvement was not obvious from a direct visual inspection of the image; however, it was clearly shown by the SNR calculations. While this may make it seem that the improvement in SNR for the HTS coil compared to the cooled copper coil was small or not significant, it should be noted that the coils were designed as simple, single-turn coils. Therefore, it could be anticipated that the construction of more complex receiving coils, such as birdcage, quadrature coils, and phased array coils, would lead to a significantly increased difference in SNR, if comparing HTS to cooled copper coils.

As described in [14], higher SNR could also be achieved using an HTS coil designed as a surface coil, but in a small area near the coil. These types of coils would find an application in MR microscopy [10], [17] or spectroscopy on high-field scanners. Cryogenic MR receiving coils can provide spatial resolution well below 100 μm in each direction of space, with acquisition times of a few minutes [18]. One of the disadvantages that prevents the wider application of cryogenic coils is the fact that they cannot be placed as close to the sample as an uncooled copper coil, because of thickness of thermal insulation. This reduces the SNR gain for cryogenic coils. However, currently, modern thermal isolation materials are available that are thin and provide a high thermal resistance at the same time. One example of such a material is aerogel.

In another study [19], an HTS surface coil was developed, with a diameter of 50 mm, designed for a high-field (1.5 T) scanner, and built from Bi-2223 material ($\text{Bi}_2\text{Sr}_2\text{Ca}_2\text{Cu}_3\text{O}_6$). Its critical temperature was 110 K. The investigators compared the HTS coil and cooled copper coil and reported an improvement in SNR by a factor of 1.11. When they compared an HTS coil and an uncooled copper coil, SNR improved by a factor of 1.36. These SNR improvements are significantly lower compared to our results. This was probably caused by the fact that the inherent noise of the receiving coil in a high-field (1.5 T) scanner does not contribute to the overall noise in the measured image as much as it does for low-field scanners. In a low-field study by Ma et al. [14], an HTS surface coil was developed and tested on a 0.2 T scanner. The measured SNR of an image acquired with this HTS coil was 1.4 times higher compared to an image measured with a cooled copper coil. This is in good agreement with our study, where we reported an SNR improvement by a factor of 1.37 with a volume coil constructed for low-field imaging.

Our study has some limitations. The width of our HTS coil was relatively small. By using wider HTS strips, the coil quality could be improved. However, our coil was compared with geometrically identical copper coils; thus, the improvement in the SNR is undeniable. The large distance between the coil and the sample also played an important role in the resultant SNR. This distance was determined by the isolation material used, which separated the insides of the cryostat at a temperature of 77 K from the area with the sample at a temperature of 296.15 K. Aerogel would seem to be a more suitable (thinner) material for thermal isolation, rather than the styrodur used. Aerogel would save about two-thirds of the insulation thickness and its thermal conductivity is approximately $0.017 \text{ W}\cdot\text{m}^{-1}\cdot\text{K}^{-1}$ instead of the $0.032 \text{ W}\cdot\text{m}^{-1}\cdot\text{K}^{-1}$ of styrodur. The use of aerogel as an isolation material could further increase the SNR gain.

Future steps would be the design of a more suitable cryostat, with closed circulation of nitrogen and better and thinner thermal isolation. Currently, different types of HTS materials, such as Hg-1223 ($\text{HgBa}_2\text{Ca}_2\text{Cu}_3\text{O}_8$), whose critical temperature is 134 K, are available. These materials need to be studied in more detail. Our next step is to test a complex receiving coil design using wider HTS tape.

5. CONCLUSION

We designed, analyzed, and experimentally verified the properties of cooled and uncooled copper and HTS receiving coils for low-field MRI as well as the influence of these coils on image quality. We demonstrated that a receiving coil built from HTS material with a dedicated preamplifier can significantly improve the SNR of the obtained image at low magnetic fields, thus time-intensive signal averaging is reduced by about a factor of 2.

Based on the results obtained, we can conclude that the HTS materials appear to be suitable for the construction of complex receiving coils, such as birdcage, quadrature coils, and phased array coils, for low-field scanners and will have applications in MR microscopy at high-field scanners as well.

ACKNOWLEDGMENT

This work was supported by the Slovak Scientific Grant Agency VEGA 2/0001/17 and by Slovak Research and Development Agency APVV-15-0029.

REFERENCES

- [1] Hoult, D.I., Richards, R.E. (1976). The signal-to-noise ratio of the nuclear magnetic resonance experiment. *Journal of Magnetic Resonance*, 24 (1), 71-85.
- [2] Hoult, D.I., Lauterbur, P.C. (1979). The sensitivity of the zeugmatographic experiment involving human samples. *Journal of Magnetic Resonance*, 34 (2), 425-433.
- [3] Ginefri, J.-Ch., Poirier-Quinot, M., Girard, O., Darrasse, L. (2007). Technical aspects: Development, manufacture and installation of a cryo-cooled HTS coil system for high-resolution in-vivo imaging of the mouse at 1.5 T. *Methods*, 43 (1), 54-67.
- [4] Schulder, M., Azmi, H., Biswal, B. (2003). Functional magnetic resonance imaging in a low-field intraoperative scanner. *Stereotactic and Functional Neurosurgery*, 80 (1-4), 125-131.
- [5] Valkovič, L., Juráš, V., Gogola, D., Frollo, I. (2012). The early effect of alcohol and caffeine on a BOLD signal measured in human hand at low-field MRI. *Applied Magnetic Resonance*, 42 (4), 463-471.
- [6] Parra-Robles, J., Cross, A.R., Santyr, G.E. (2005). Erratum: "Theoretical signal-to-noise ratio and spatial resolution dependence on the magnetic field strength for hyperpolarized noble gas magnetic resonance imaging of human lungs" [Med. Phys. 32, 221-229 (2005)]. *Medical Physics*, 33 (5), 1525-1526.
- [7] Vojtíšek, L., Frollo, I., Valkovič, L., Gogola, D., Juráš, V. (2011). Phased array receiving coils for low field lungs MRI: Design and optimization. *Measurement Science Review*, 11 (2), 61-66.
- [8] Redpath, T.W. (1998). Signal-to-noise ratio in MRI. *The British Journal of Radiology*, 71, 704-707.
- [9] Lee, H.-L., Lin, I.-T., Chen, J.-H., Horng, H.-E., Yang, H.-C. (2005). High- T_c superconducting receiving coils for nuclear magnetic resonance imaging. *IEEE Transactions on Applied Superconductivity*, 15 (2), 1326-1329.
- [10] Miller, J.R., Hurlston, S.E., Ma, Q.Y., Face, D.W., Kountz, D.J., MacFall, J.R., Hedlund, L.W., Johnson, G.A. (1999). Performance of a high-temperature superconducting probe for in vivo microscopy at 2.0 T. *Magnetic Resonance in Medicine*, 41 (1), 72-79.
- [11] Cheng, M.-Ch. (2004). *High temperature superconductor tape RF volume coil for MRI systems*. Thesis, The University of Hong Kong.
- [12] Giovannetti, G., Francesconi, R., Landini, L., Santarelli, M.F., Positano, V., Viti, V., Benassi, A. (2004). Conductor geometry and capacitor quality for performance optimization of low-frequency birdcage coils. *Concepts in Magnetic Resonance B*, 20B (1), 9-16.
- [13] Mispelter, J., Lupu, M., Briguet, A. (2006). *NMR Probeheads: For Biophysical and Biomedical Experiments*, 1st Edition. Imperial College, 596.
- [14] Ma, Q.Y., Chan, K.C., Kacher, D.F., Gao, E., Chow, M.S., Wong, K.K., Xu, H., Yang, E.S., Young, G.S., Miller, J.R., Jolesz, F.A. (2003). Superconducting RF coils for clinical MR imaging at low field. *Academic Radiology*, 10 (9), 978-987.
- [15] Nouls, J.C., Izenon, M.G., Greeley, H.P., Johnson, G.A. (2008). Design of a superconducting volume coil for magnetic resonance microscopy of the mouse brain. *Journal of Magnetic Resonance*, 191 (2), 231-238.
- [16] Cheng, M.C., Lee, K.H., Chan, K.C., Wong, K.K., Yang, E.S. (2003). HTS tape RF coil for low field MRI. In *Proceedings of the International Society for Magnetic Resonance in Medicine*, Toronto, Ontario, Canada, 2359.
- [17] Ginefri, J.-Ch., Darrasse, L., Crozat, P. (2001). High-temperature superconducting surface coil for in vivo microimaging of the human skin. *Magnetic Resonance in Medicine*, 45 (3), 376-382.
- [18] Darrasse, L., Ginefri, J.-Ch. (2003). Perspectives with cryogenic RF probes in biomedical MRI. *Biochimie*, 85 (9), 915-937.
- [19] Yuan, J., Shen, G.X., Wang, Ch., Wu, B., Qu, P. (2004). Use of Bi-2223 multifilamentary tapes as RF coils for 1.5 T MRI application. *Physica C*, 415 (4), 189-196.

Received January 16, 2018.

Accepted April 25, 2018.